Expanded View Figures

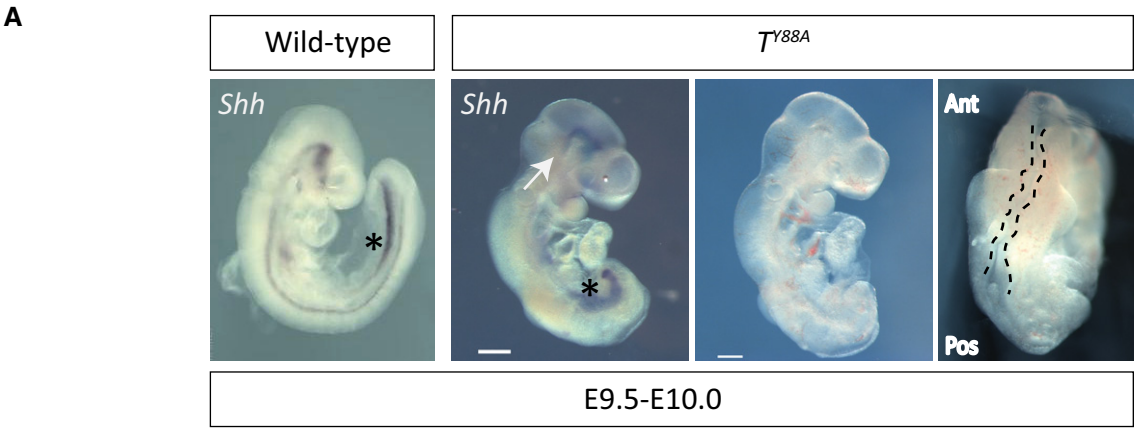

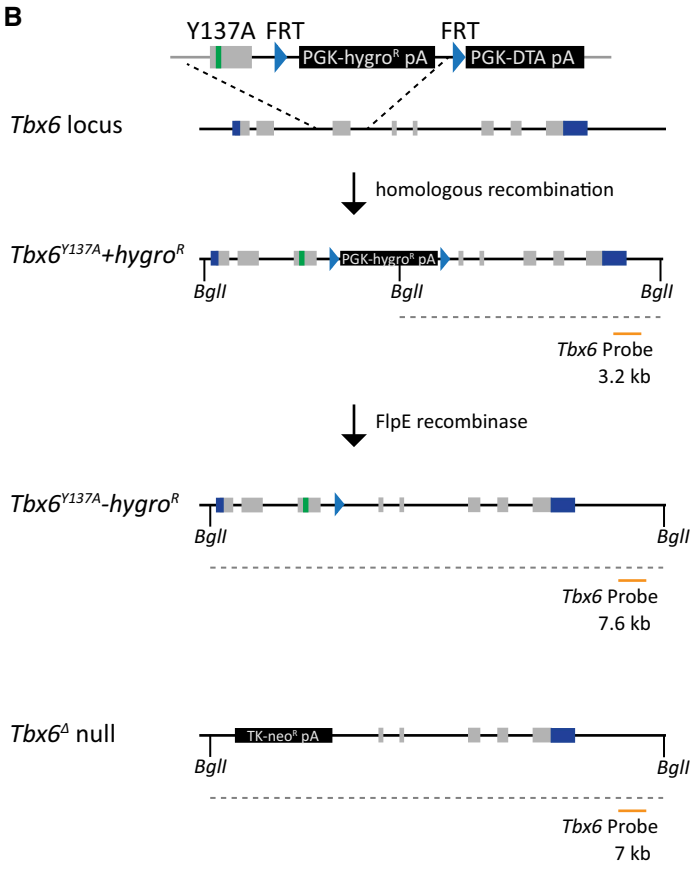

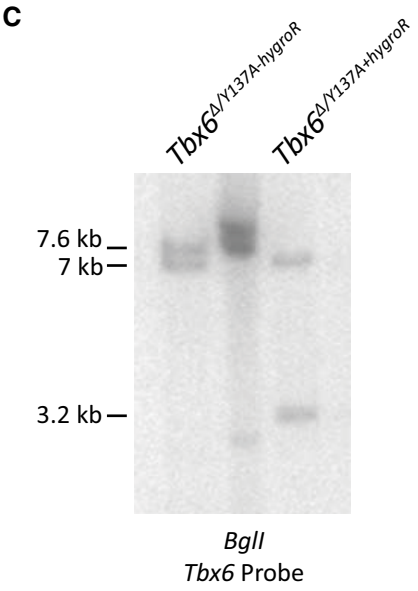

Figure EV1.

Figure EV1. Y to A mutations in *T* and *Tbx6*.

A Whole-mount *in situ* hybridization for *Shh* expression reveals the loss of notochordal structures in T^{Y88A} mutant embryos at E9.5–10.0. White arrows point to the remnants of notochord at the rostral end of the embryo. Asterisks depict *Shh* staining in the foregut. The panels on the right display the kinked neural tube (outlined with a black dashed line) and truncated posterior mesoderm in the T^{Y88A} mutant embryos at E9.5. The T^{Y88A} mutant embryo is the same as that in Fig 1F. Scale bar: 200 μm. Ant, anterior; Pos, posterior.

B Schematic illustrating the homologous recombination strategy to insert the Y137A point mutation in the endogenous *Tbx6* locus. The hygromycin selection was removed by expression of *FlpE* recombinase. The orange line depicts the probe used for Southern blotting to confirm integration of the mutation and removal of the hygromycin resistance cassette. *BglI* restriction enzyme sites used for Southern blotting are depicted.

C Southern blot of mESC genomic DNA to detect homologous recombination of the Y137A mutation and removal of the hygromycin cassette using the probe depicted in (B). The 3.2-kb band corresponds to the $Tbx6^{Y137A}$ mutant allele containing the hygromycin selection cassette, while the 7.6-kb band corresponds to the $Tbx6^{Y137A}$ allele with the selection cassette removed. The 7.0-kb band corresponds to the $Tbx6^{\Delta}$ null allele.

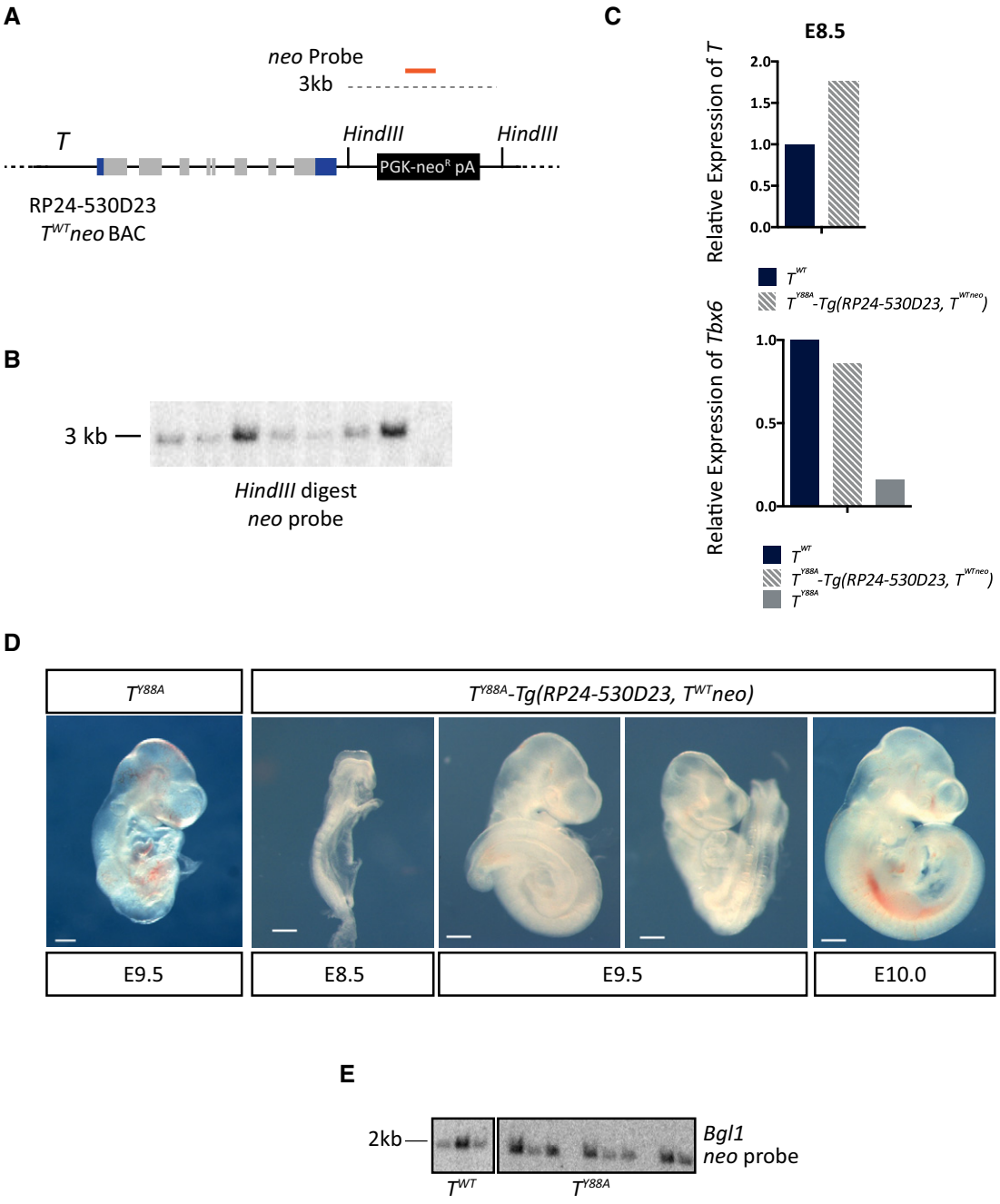

Figure EV2. The *T* BAC is able to rescue the T^{Y88A} mutant phenotype.

A Schematic illustrating the wild-type RP24-530D23-T^{WT}*neo* BAC, containing a neomycin selection cassette recombined into the BAC backbone. The orange line depicts the probe used to confirm genomic integration of the T^{WT}*neo* BAC by Southern blot. Restriction enzyme sites used for Southern blotting are also depicted.

B Southern blot of genomic DNA from T^{Y88A} mESC clones in which the T^{WT}*neo* BAC was randomly integrated. Positive clones display a band at 3 kb when using a probe against the neomycin resistance gene.

C RT–qPCR analysis of *T* and *Tbx6* expression in whole embryos at E8.5 reveals that *T* expression and *Tbx6* expression are rescued in T^{Y88A}-*Tg*(*RP24-530D23*, T^{WT}*neo*) embryos.

D Bright field images of T^{Y88A}-*Tg*(*RP24-530D23*, T^{WT}*neo*) embryos from E8.5 to E10.0 reveals rescue of gross morphological phenotypes when compared to the T^{Y88A} mutant. Scale bar: 200 μm.

E Southern blot of genomic DNA from T^{WT} and T^{Y88A} mESC clones in which the $T^{mCherry}$ reporter BAC was randomly integrated. Positive clones display a band at 2 kb when using a probe against the neomycin resistance gene.

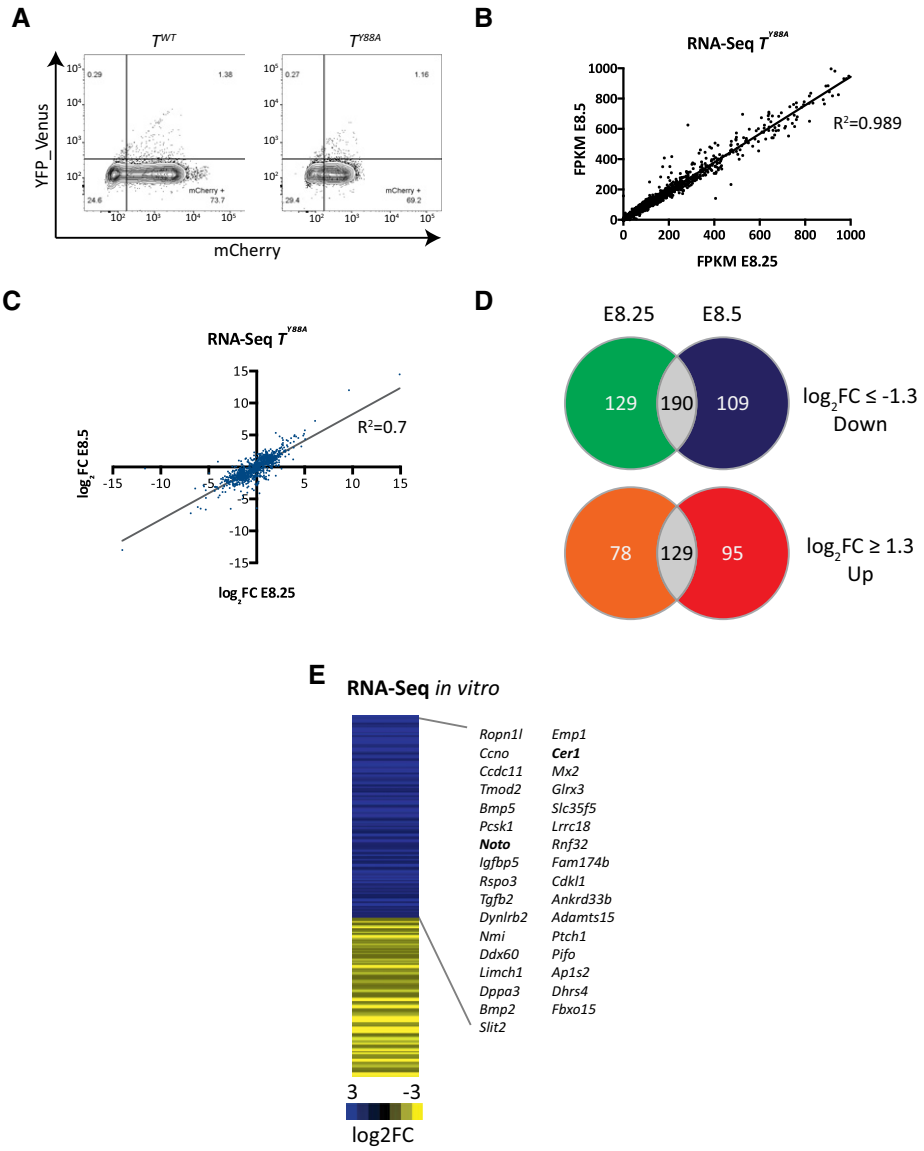

Figure EV3. Transcriptome analysis in T^{Y88A} mutants *in vivo*.

A FACS plots from the sorting of T-mCHERRY-positive cells from T^{WT} and T^{Y88A} embryos for RNA-seq.

B Scatter plot of FPKM values from RNA-Seq using mesodermal cells of T^{Y88A} embryos at E8.25 and E8.5 (one biological replicate for each timepoint).

C Scatter plot of $\log_2$ fold change values comparing T^{Y88A} mutant mesodermal cells to T^{WT} at E8.25 and E8.5 ($\log_2$ fold change $\geq$ 1.3).

D Venn diagrams illustrating genes that are dysregulated both at E8.25 and E8.5 in T^{Y88A} mutant mesodermal cells compared to T^{WT} ($\log_2$ fold change $\geq$ 1.3).

E Heat map depicting dysregulated gene expression ($\log_2$ fold change $\geq$ 1.3) in T^{Y88A} mesodermal cells differentiated *in vitro* compared to T^{WT} from RNA-Seq of one biological replicate. Gene names correspond to genes that are downregulated and contain a nearby TBS with reduced H3K27ac (fold change > 1.4). Bold gene names indicate known T targets.

Figure EV4. Disruption of H3K27ac at TBS in the T^{Y88A} mutant.

A MA plots of H3K27me3 ChIP-Seq (one biological replicate) read density ±1 kb from transcriptional start sites (TSS, with TBS removed) and TBS. Blue and red lines depict fold change values of −1.4 and 1.4, respectively. The percentage of regions above and below this threshold (red and blue, respectively) are indicated on the plots.

B MA plot of H3K27ac ChIP-seq (one biological replicate) read density ±1 kb from T binding sites and TSS (with TBS removed) in T^{WT} versus T^{Y88A} mutant mesodermal cells differentiated *in vitro*. Blue and red lines depict fold change values of −1.4 and 1.4, respectively. The percentage of regions above and below this threshold (red and blue, respectively) are indicated on the plots.

C Overlap of TBS with higher H3K27me3 and lower H3K27ac (fold change > 1.4) from one biological ChIP-Seq replicate each.

D Genomic distribution of TBS with lower H3K27ac (fold change > 1.4).

E MA plots of H3K27ac read density ±1 kb from TBS regions that overlap K4me1 peaks. Blue and red lines depict fold change values of −1.4 and 1.4, respectively. The percentage of regions above and below this threshold (red and blue, respectively) are indicated on the plots.

F Statistical overrepresentation test (PANTHER) of GO terms from genes nearby regions of lower H3K27ac in T^{Y88A} mutant mesodermal cells differentiated *in vitro* (fold change > 1.4 when compared to T^{WT}). Gray bars indicate fold enrichment over the reference *Mus musculus* gene list.

G Genome browser tracks depicting T binding in mesodermal cells differentiated *in vitro*, and H3K27ac and H3K27me3 at TBS of target genes.

H Venn diagram illustrating the overlap between downregulated gene expression from RNA-Seq *in vivo* ($\log_2$ fold change ≥ 1.3) and the neighboring two to three genes from each TBS with reduced H3K27ac (fold change > 1.4) from one biological ChIP-Seq replicate. The lower Venn diagram illustrates the overlap between downregulated gene expression from RNA-Seq from *in vitro*-differentiated mesodermal cell ($\log_2$ fold change ≥ 1.3) and the neighboring two to three genes from each TBS with reduced H3K27ac (fold change > 1.4).

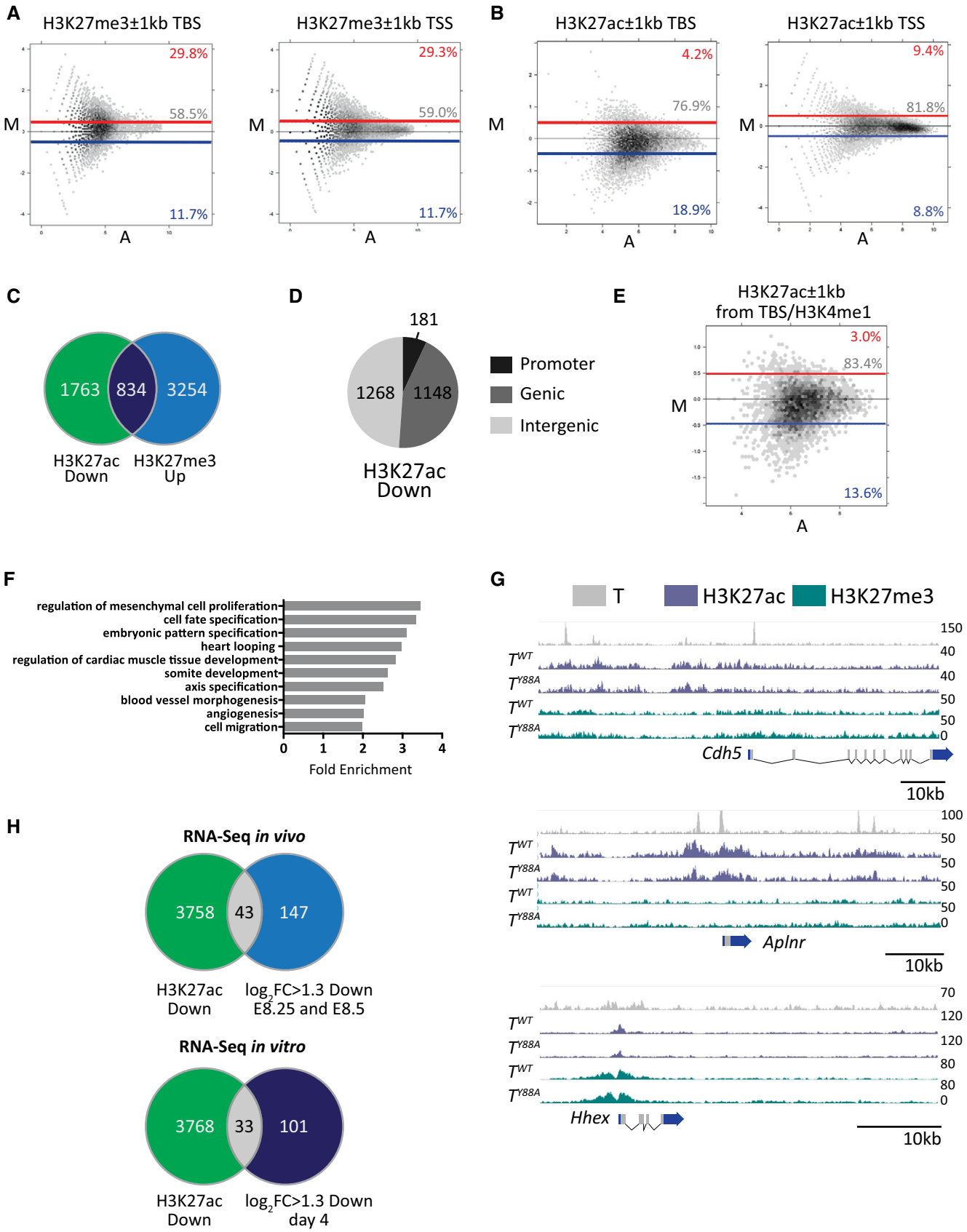
A
H3K27me3±1kb TBS
29.8%
58.5%
11.7%
M
A
H3K27me3±1kb TSS
29.3%
59.0%
11.7%
B
H3K27ac±1kb TBS
4.2%
76.9%
18.9%
H3K27ac±1kb TSS
9.4%
81.8%
8.8%
C
1763
834
3254
H3K27ac Down
H3K27me3 Up
D
181
1268
1148
H3K27ac Down
Promoter
Genic
Intergenic
E
H3K27ac±1kb from TBS/H3K4me1
3.0%
83.4%
13.6%
F
regulation of mesenchymal cell proliferation
cell fate specification
embryonic pattern specification
heart looping
regulation of cardiac muscle tissue development
somite development
axis specification
blood vessel morphogenesis
angiogenesis
cell migration
0 1 2 3 4
Fold Enrichment
G
T
H3K27ac
H3K27me3
Cdh5
Aplnr
Hhex
10kb
H
RNA-Seq in vivo
3758
43
147
H3K27ac Down
log2FC>1.3 Down E8.25 and E8.5
RNA-Seq in vitro
3768
33
101
H3K27ac Down
log2FC>1.3 Down day 4

Figure EV4.

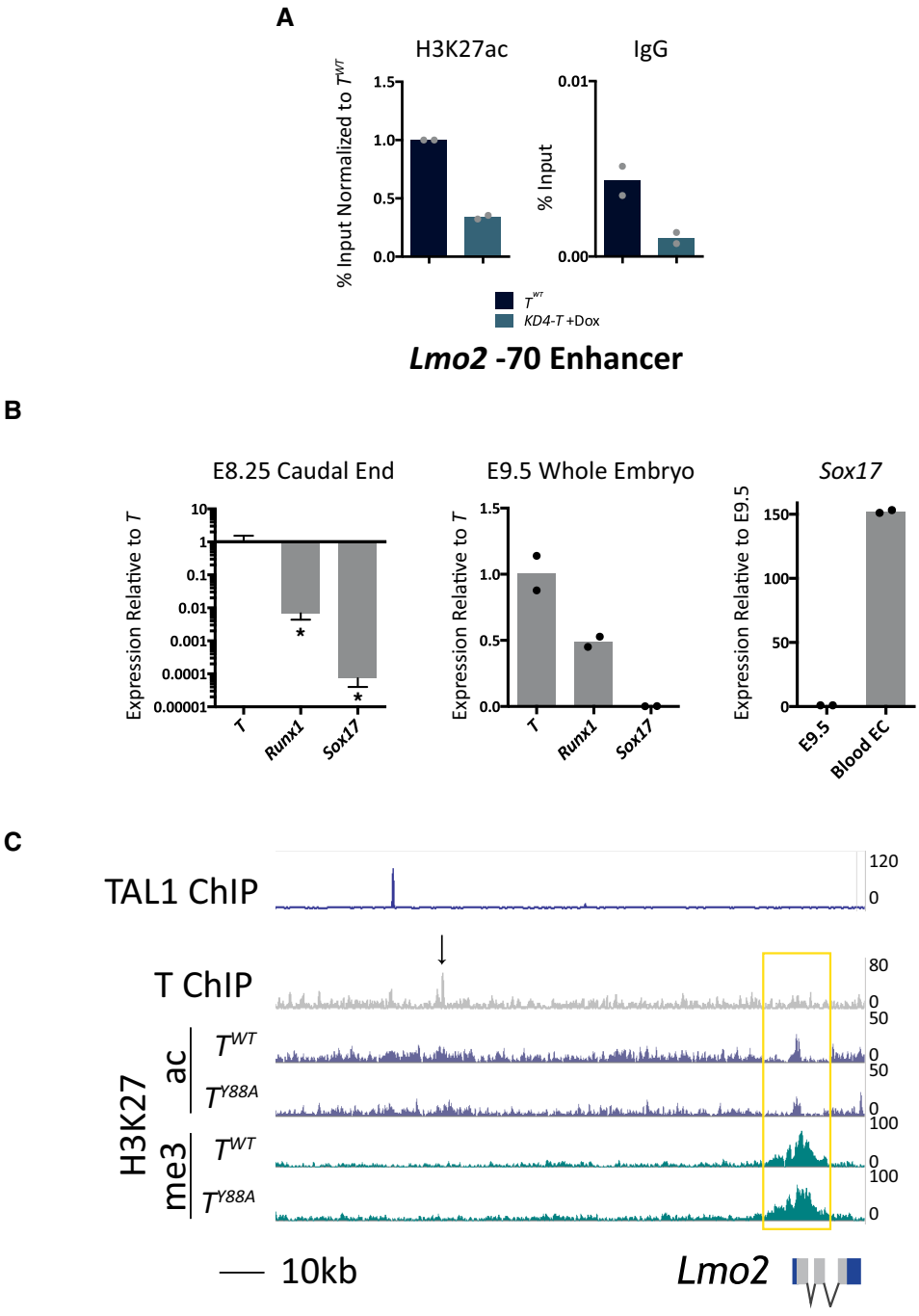

Figure EV5. T regulation of the *Lmo2* locus.

A ChIP-qPCR analysis of H3K27ac at the *Lmo2* −70 enhancer in *KD4-T in vitro*-differentiated mesodermal cells at day 4. The mean of $n = 2$ biological replicates is depicted.

B RT-qPCR analysis of *T*, *Runx1*, and *Sox17* expression in E8.25 caudal ends of T^{WT} embryos. Levels of *Runx1* and *Sox17* are significantly lower than that of *T* in E8.25 caudal ends. Error bars depict SD of $n = 3$ biological replicates. *$P < 0.02$ using an unpaired *t*-test. Middle graph depicts *T*, *Runx1*, and *Sox17* levels in whole E9.5 embryos as a positive control for the qPCR primers. The mean of $n = 2$ biological replicates is depicted. *Sox17* expression is low in E9.5 embryos, and the graph on the right depicts high *Sox17* expression in $CD31^+$ blood endothelial cells isolated from embryonic skin at E15.5. The mean of $n = 2$ biological replicates is depicted.

C Genome browser tracks of the *Lmo2* genomic locus with T, H3K27ac, and H3K27me3 tracks from the ChIP-Seq analysis in this study. TAL1 ChIP-Seq tracks were depicted using data from [45], and illustrate TAL1 binding in mesodermal cells at the *Lmo2* −75 enhancer, approximately 7 kb upstream of T binding at the −70 enhancer. The black arrow indicates the region removed by CRISPR/Cas9-mediated genome editing at the TBS of the *Lmo2* −70 enhancer.